

## **Monitoring And Optimization Of Drilling Process Parameters Using Gaintegrated With Semi-Empirical Method And Hole Quality**

**Nakandhra kumar R. S.<sup>1</sup> , Balaji Ramachandran<sup>2</sup> , V. Parthasarathy<sup>3</sup> , Vasudev K. L.<sup>4</sup> , C. Edwin Samuel<sup>5</sup> , Anirudh Srinivas Vellimedu<sup>6</sup>**

<sup>1</sup>Centre for Automation and Robotics, Department of Mechanical Engineering, Hindustan Institute of Technology and Science, Chennai, India.

<sup>2</sup>NoobTron Private Limited, Chennai-600064, India.

<sup>3</sup>Department of Physics, Hindustan Institute of Technology and Science, Padur, Chennai, India

<sup>4</sup>Department of Mechanical Engineering, Amrita School of Engineering, Chennai, Amrita Viswa Vidyapeetham, India.

<sup>5</sup>Hokkaido University, Department of Mechanical and Space Engineering, Computational Fluid Mechanics Lab, Sapporo, Hokkaido Japan 060-0808

<sup>6</sup>Department of Mechanical Engineering, Sri Sairam Engineering College, Chennai, India

---

### **Abstract**

Cutting parameters in drilling operations have a significant impact on drill wear and workpiece dimension changes. The work presented here deals with the optimization of cutting parameters in drilling operations to minimize flank wear to utilize long life. The optimization model utilizes genetic algorithm. In the present model, drilling process parameters (i.e. cutting speed ( $v$ , rpm), feed ( $f$ ,

mm/min), depth of cut ( $d$ , mm) and torsional-axial amplitude ratio ( $T_{p1}/T_{p2}$ ) are considered as variables. A semi-empirical relation between the variables and flank wear is derived by conducting experiments followed by regression analysis. The derived semi-empirical relation is then used in the optimization process to find the optimum parameters. The results are validated by conducting more experiments. The reported results show that for the given bounds on the variables, the optimization framework is able to produce drilling parameters with minimum flank wear and extension of life of drill tool decided through monitoring hole quality by Surtronic 182 surface roughness measurement.

**Keywords:** Drilling, tool wear, genetic algorithm, torsional-axial vibrations, surface roughness

---

## Introduction

Monitoring tool wear and the cutting area during the drilling process is not easy: The development of robust and semi-empirical methods to make the drilling operation a fully automated machining process is therefore desirable [1]. The literature has identified two possible ways of utilizing tools that affect the drilling process: (a) underutilization of a tool which results in frequent tool change and longer machine downtime, thereby reducing the system productivity and increasing the cost. (b) over utilization of a tool, which affects, the work-piece quality, surface finish and dimensions and disrupts the automated drilling process. From these studies, one can conclude that tool condition monitoring systems are imperative for the measurement of the progress of tool wear along with surface roughness measurement.

Kaye et al. developed a unique technique for on-line prediction of tool flank wear in turning using spindle speed changes. An optical encoder was mounted on the spindle shaft and interfaced with an IBM compatible

microcomputer [2]. The varying spindle speeds were compensated for lathe transmission ratio, the electrical configuration of the lathe's motor and the torque-speed relationship of the machine. Cus et al. concluded that mathematical model development using cutting conditions required for complex optimization of the machining process in the right way leads to product quality via a process quality [3]. Ertunc and Loparo proposed methods to monitor on-line tool wear conditions in drilling operations. The proposed monitoring methods use information about force signals (thrust and torque) and power signals (spindle and servo). They concluded the work by stating that Hidden Markov Models offer a promising approach to monitor real-time drilling operations [4].

Jen et al. studied the torsional–axial effect during drilling. The effect manifests itself during the material removal processes as plastic deformation of the workpiece and friction at the drill-chip interface [5]. Roukema and Altintas developed a mathematical model of the torsional-axial chatter vibrations in drilling. The drill was modeled as a pre-twisted beam that exhibits axial deflections due to torque and thrust loading. A mechanistic cutting force model was used to model the thrust and the torque as functions of the cutting parameters namely, feed rate, speed, radial depth of cut and drill geometry [6]. Al-Sulaiman et al. developed a reliable method for online tool condition monitoring. The power required to run the spindle motor was nullified and only the power for actual drilling was noted. The effects of drill diameter, speed and feed rate on tool wear during drilling was studied [7]. Brozek determined the relationship between tool life and cutting speed through cutting condition optimization for achieving a minimum production cost criterion. The developed mathematical models for the surface

roughness using response surface methodology. Author have concluded and listed that the parameters cutting velocity, feed, rake angle and nose radius of the cutting tool affects the surface finish [8].

Roukema and Altintas developed a time-domain model of the torsional-axial vibrations in drilling. The drill rotates and feeds axially into the workpiece while the structural vibrations are excited by the cutting torque and thrust [6]. The drill edge location has been predicted using the kinematics model, and the generated surface is digitized at discrete time intervals. The distribution of chip thickness, which is affected by both rigid body motion and structural vibrations, is evaluated by subtracting the presently generated surface from the previous one. The model also considers cutting coefficient nonlinearities, tool jumping out of cut and overlapping of multiple regeneration waves. Teti et al. reviewed the present trends in sensor monitoring of machining operations. They concluded that very few achievements found actual application because of the difficulty, sophisticated usage of these techniques and methods [11]. The main challenges of machining process monitoring systems are the development of algorithms and paradigms based on wavelet transform, neural networks, etc. really autonomous from machine tool operators

Agrawal et. al. have compared influence of cutting conditions on surface roughness with mathematical model obtained through regression models [15]. Ratava et al. (2017) discussed a model to classify tool breakage based on the depth of cut, the feed rate and an estimate of tool displacement. They concluded that the method was

relatively simple and classified correctly over 80% of the experimental samples [12-13], The prospects for a real-time implementation of the method are promising. However, notable cluster of failures was the combination of high cutting speed with a low depth of cut. Antic et al. developed a tool wear monitoring strategy that relies on novel texture-based descriptors. They consider the module of the Short Term Discrete Fourier Transform spectra obtained from the particular vibration sensors signal utterance as the 2D textured image. They validated this methodology by conducting experiments on real-time TCM system [13].

EN24 steel with 40% carbon content is widely used in machinery, automobile and aero components such as brake drums and sprocket wheels due to its specific properties such as abrasion resistance, high toughness, improved fatigue strength and capability of operating at elevated temperatures [14-15]. However, drilling operations are tremendously challenging as variation in the cutting parameters leads to an increase in heat around the cutting edge of the drill. It may subsequently cause the drill to abruptly change its status and leads to the failure of the cutting tool. Hence, drilling of hard materials more than the expected periodtime of replacement can possibly be accomplished through optimum cutting parameters. The present work is motivated by this premise. A Genetic Algorithm (GAs) has been implemented to optimize the drilling process parameters along with the torsional-axial amplitude ratio to minimize the flank wear.

GAs are adaptive heuristic search algorithms Deb (2014). GAs are based on the concept of natural selection and

genetics. They solve optimization problems by intelligently exploiting random search methods. Even though they use random numbers, GAs are by no means random themselves; instead, they use the information from the previous generation to direct the search into the region of better performance within the search space. GAs follow the principle of 'survival of the fittest'. GAs can solve multi-objective, single objective, multi-variable, multi-constraint problems and also problems with multiple solutions. Since GAs are independent of the type of objective function, they can be implemented in solving multi-dimensional, non-differential, non-continuous and even non-parametric problems. GAs may offer a solution where typical search and optimization techniques, such as linear programming and others fail for problems dealing with a large state-space, a multi-modal state-space, or n-dimensional surface: see Vasudev et al. Surface quality is evaluated through surface roughness measurement most accepted approach by Joshi et. al [16-21]. This paper utilizes GAs approach for identifying suitable cutting conditions during drilling hard materials. Further the parameters are monitored through received vibration signals in Sound and Vibration software of LabView and workpiece hole quality through measurement of surface roughness. The following sections are detailing about Basic formulation of the mathematical model, Optimization problem, Solution by GA, Experimental setup and optimization results.

### **Basic formulation of the mathematical model**

The 27 experimental datasets reported in the author's previous work have been used to form a mathematical model based on multiple regression analysis (using the least square method). Friedman and Field (1974) have suggested a relationship between the cutting tool life (T) and the cutting independent process parameters speed

of cut ( $v$ , rpm), feed rate ( $f$ , mm/min), and depth of cut ( $d$ , mm) using Taylor's equation as follows:

$$T = \beta_0 v^{p_1} f^{p_2} d^{p_3} \quad (1)$$

where  $\beta_0$  is a coefficient and  $p_1$ ,  $p_2$ , and  $p_3$  are constants that depend on the mechanical properties of the material being machined. Following Taylor's equation, one can form a relation for wear on the flank is proportional to the area of flank wear scar at time  $t$  can be expressed as

$$W = W_0 + \Delta W \quad (2)$$

where  $W_0$  is the initial wear,  $\Delta W$  is the increase in wear and can be given as  $\Delta W = \beta_0 v^{p_1} f^{p_2} d^{p_3} t^{p_4}$ ,  $v$ ,  $f$ , and  $d$  are the cutting speed, feed rate and depth of cut respectively. Following the process as mentioned in Nakandhrakumar et al. [18], the following relationship between flank wear and vibration amplitude ratio has been derived

$$W = 0.04 \left( \frac{T_{p1}}{T_{p2}} \right)^{0.58} + 0.0000016 v^{1.13} f^{0.92} d^{1.052} \quad (3)$$

Eq(3) has been programmed in Matlab and calculated the flank wear values for the set of variables considered in the 27 experiments. The comparison with experimental values of flank wear with the Eq(3) has a mismatch with a certain set upto 55%. Therefore, it is necessary to relook the formulation, to reduce the error. After some mathematical manipulations, we conclude that the following equation for flank wear performs better than Eq(3).

$$W = 0.0107 \left( \frac{T_{p1}}{T_{p2}} \right)^{0.58} + 0.0000638 v^{1.128} f^{0.92} d^{1.092} \quad (4)$$

### **Optimization Problem**

The optimization problem treated in this paper consists of minimization of flank wear subject to constraints on drilling process parameters and vibration amplitude ratio. Eq (4) has been used to compute the objective function which is flank wear. The problem may be stated as follows:

Minimize  $F = W (T_{p1}/T_{p2}, v, f)$  subject to constant  $d = 11\text{mm}$

$x_1 = T_{p1}/T_{p2}$  (Amplitude ratio Torsional-axial vibrations amplitude)

$x_2 = v$  (Cutting Speed, rpm)

$x_3 = f$  (Feed, mm/min)

$x_4 = d$  (depth of cut, mm)

and

$x_{L1} = 20, x_{L2} = 800, x_{L3} = 0.07, x_{L4} = 11, x_{U1} = 100, x_{U2} = 1000, x_{U3} = 0.12, x_{U4} = 11$

where  $x_{Li}, x_{Ui}$  are the lower and upper bounds of the  $i$ th variable

### **Solution by GA**

The flowchart in Figure (1) provides an overview of GA-based optimization. The method, specialized to the problem described above is discussed below.

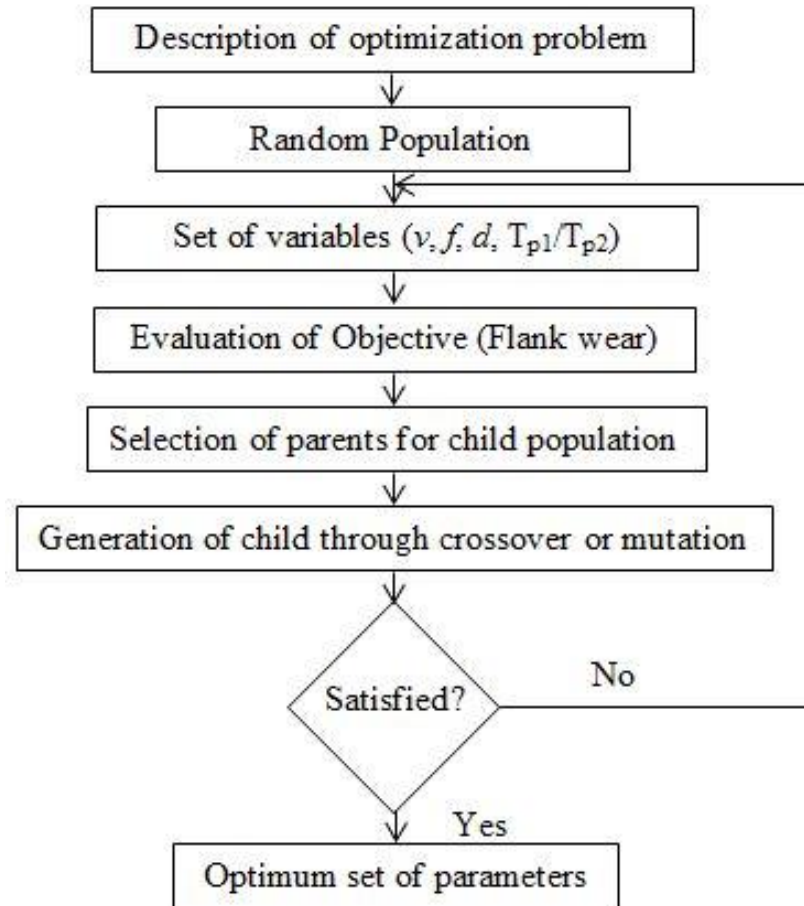


Figure 1: Flow chart of complete optimization process

**Step1:** Generate Initial Configurations

A set of p initial population  $C^{(i)}$  will be generated using

$$x_i^{(j)} = x_{Li} + \alpha(x_{Ui} - x_{Li}) \quad (5)$$

where  $p$  is population size (=100),  $\alpha$  is a random number between 0 and 1, generated every time Equation(5) is used. In other words, the application of this equation requires the generation of  $4p$  random numbers  $\alpha$ .

### **Step 2:** Sort Initial Configurations

Compute the flank wear  $W^{(j)}$  using Equation (4) of each of these  $p$  and arrange these configurations using 'non-dominated sorting' technique (Deb 2014). This set of configurations -after sorting is called the parent population.

### **Step 3:** Tournament Selection

Tournament selection involves randomly choosing  $k$  numbers between 1 and  $p$  and then choosing the minimum of those  $k$  numbers. Typically,  $k = 4$  is adopted. To this end, four random numbers  $\beta_k$  ( $k = 1, \dots, 4$ ) between 0 and 1 are generated and used to calculate  $q_k = \text{ceil}(p\beta_k)$  where  $\text{ceil}(x)$  sets  $x$  to the nearest integer towards infinity. The result of tournament selection is  $T = \min(q_1, q_2, q_3, q_4)$ . This process is repeated  $p$  times to obtain the tournament selection vector.

### **Step 4:** Generate Child Population

Generate once again a random number  $\alpha$  between 0 and 1.

#### 4.1 Crossover

If  $\alpha \leq \bar{\alpha}$  then generate two new configurations using

$$\delta_i = (2\gamma_i)^{\frac{1}{\eta+1}} \text{ (if } \gamma_i < 0.5\text{); } \delta_i = 1/[2(1 - \gamma_i)]^{\frac{1}{\eta+1}} \text{ (if } \gamma_i \geq 0.5\text{)} \quad (6)$$

$$l = l + 1; x_i^{(l)} = \frac{1}{2}\{(1-\delta_i)x_i^{(q1)} + (1+\delta_i)x_i^{(q2)}\} \text{ exit step 4 if } l = p \quad (7)$$

$$l = l + 1; x_i^{(l)} = \frac{1}{2}\{(1+\delta_i)x_i^{(q1)} + (1-\delta_i)x_i^{(q2)}\} \text{ exit step 4 if } l = p \quad (8)$$

Where  $\gamma_i$  ( $i = 1,2,3$ ) random numbers generated each time Equations (6, 7, 8) are used. Clearly, if there are four variables, i.e.  $N = 8$ , one would need 8 values of  $\gamma_i$  for these two configurations. We will repeat this step until the number of configurations generated is equal to the size  $p$ .

#### 4.2 Mutation

If  $\alpha \geq \bar{\alpha}$  then generate a new configuration using

$$\delta_i = (2\gamma_i)^{\frac{1}{\eta+1}} - 1 \text{ (if } \gamma_i < 0.5\text{); } \delta_i = 1 - [2(1 - \gamma_i)]^{\frac{1}{\eta+1}} \text{ (if } \gamma_i \geq 0.5\text{)} \quad (9)$$

$$l = l + 1; x_i^{(l)} = x_i^{(q1)} + \delta(x_{Ui} - x_{Li}) \text{ exit step 4 if } l = p \quad (10)$$

Where  $\bar{\alpha} = 0.8$  and  $\eta = 20$  have been used in this work. At the end of step 4, we have  $p$  new configurations called child population.

### **Step 5:**

Compute the flank wear  $W^{(i)}$  of each of these  $p$  new configurations and construct a set of  $2p$  configurations by appending the new set in Step 4 to the set in Step 1. And reorder these  $2p$  configurations as was done in Step 2 and consider the first  $p$  configurations and remove the rest. With these new  $p$  configurations go to Step 3 and proceed for next iteration till the flank wear of the first configuration, does not decrease further with an assumed tolerance. This will then be the best configuration.

### **Experimental setup**

An illustrative representation of the experimental set-up is reported in Figure (2). The experimental set-up used in this work is similar to that of the one reported in the author's previous work. ACE Micromatic CNC Vertical Machining center as shown in Fig.2 has been used in this study in contrast to the 3 HP, HAAS machine without coolant [19, 22]. To verify the results of the optimization simulation, we considered a circular workpiece of material AISI 1040 carbon steel with 120 mm diameter and 11 mm thickness. The chemical composition and material properties have been reported in Tables 1 and 2 respectively. The samples were maintained with the hardness of 30.9 HRC. High-speed steel (HSS) twist drill of 6 mm diameter was used. The geometry of the drill bit is listed in Table 3 and its chemical composition is listed in Table 4. All experiments were carried out under dry cutting without coolant conditions. A special CNC program was run to track vibration signals as a function of wear. The vibration signals were measured in (transverse) Y-direction using Kistler (8636C50 model)

accelerometer sensor which is positioned at the center of the plate for all drilling operations of Pitch Circle Diameter (PCD) 60.

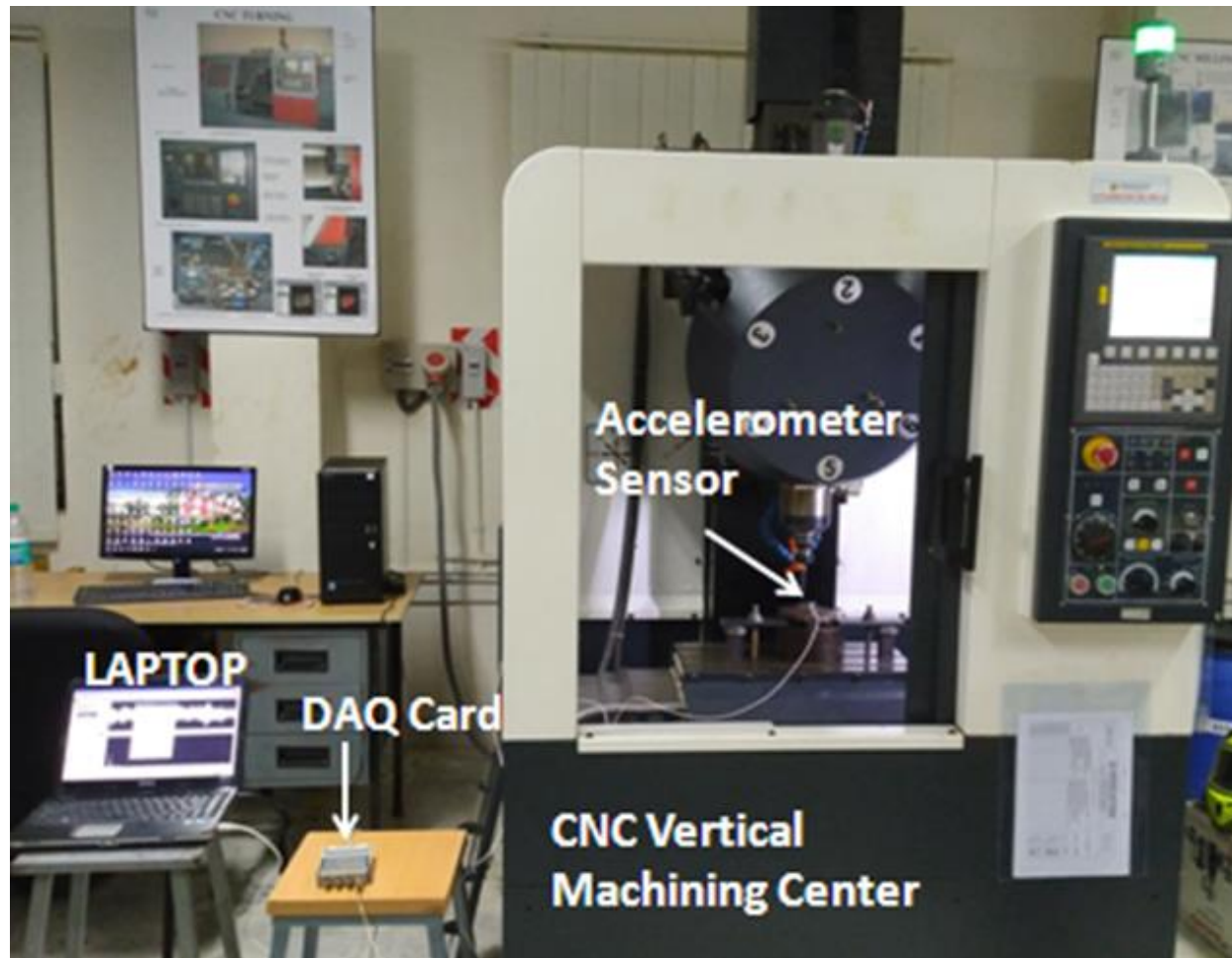


Figure 2: Illustration of Experimental setup

**Table 1:** Chemical composition of the workpiece

| Chemical composition | C    | Ni  | Cr   | Mo  | S     | Mg  | Si   | P     |
|----------------------|------|-----|------|-----|-------|-----|------|-------|
| Weight %             | 0.38 | 1.3 | 1.02 | 0.2 | 0.047 | 0.2 | 0.25 | 0.034 |

**Table 2:** Workpiece Mechanical properties

| Tensile strength (MN/m <sup>2</sup> ) | Yield stress (MN/m <sup>2</sup> ) | Density (Kg/m <sup>3</sup> ) | Elongation (%) | Brinell Hardness |
|---------------------------------------|-----------------------------------|------------------------------|----------------|------------------|
| 905                                   | 742                               | 7430                         | 4.64           | 284              |

**Table 3:** HSS drill geometric parameters

|                 |             |
|-----------------|-------------|
| Drill diameter  | 6           |
| Flute length    | 57          |
| Overall length  | 93          |
| Point angle (°) | 118         |
| Helix angle (°) | 25          |
| Flutes/Flute    | 2/Parabolic |
| Shank type      | Straight    |

**Table 4:** Chemical composition of HSS drill materials

| Chemical composition | W | Mo | Cr | V | C | Mn | Si | Cu | Pb | Ni | P | S | Al | Ti |
|----------------------|---|----|----|---|---|----|----|----|----|----|---|---|----|----|
|                      |   |    |    |   |   |    |    |    |    |    |   |   |    |    |

|          |       |       |       |      |     |       |      |       |       |       |       |       |      |       |
|----------|-------|-------|-------|------|-----|-------|------|-------|-------|-------|-------|-------|------|-------|
| Weight % | 6.169 | 5.057 | 4.198 | 1.97 | 0.9 | 0.363 | 0.24 | 0.175 | 0.073 | 0.055 | 0.016 | 0.015 | 0.07 | 0.009 |
|----------|-------|-------|-------|------|-----|-------|------|-------|-------|-------|-------|-------|------|-------|

Data acquisition card (NI-DAQ 9133) is used to convert the received analog vibration signals into digital signals with a sampling of 25 kHz and interfaced with a personal computer. The signals once received in the computer system will be processed using LabVIEW software to track the torsional-axial vibration amplitudes. The machine was stopped after drilling till the vibration amplitude ratio values match with that of the optimum value and the drill bit will be removed from the spindle to measure the flank wear using the tool maker's microscope (Model 176-811E) at 15× magnification. The flank wear will be calculated as the average of the measured values at 4 locations on the drill bit (2 on each side) as shown in Figure (3). The entire process of the experiment has been presented in a block diagram in Fig. (4)

The number of experiments was reduced to 4 in this work as we are validating only the results from the optimization process. A detailed study on the formation of semi-empirical relation between tool flank wear and drilling parameters has been carried out.

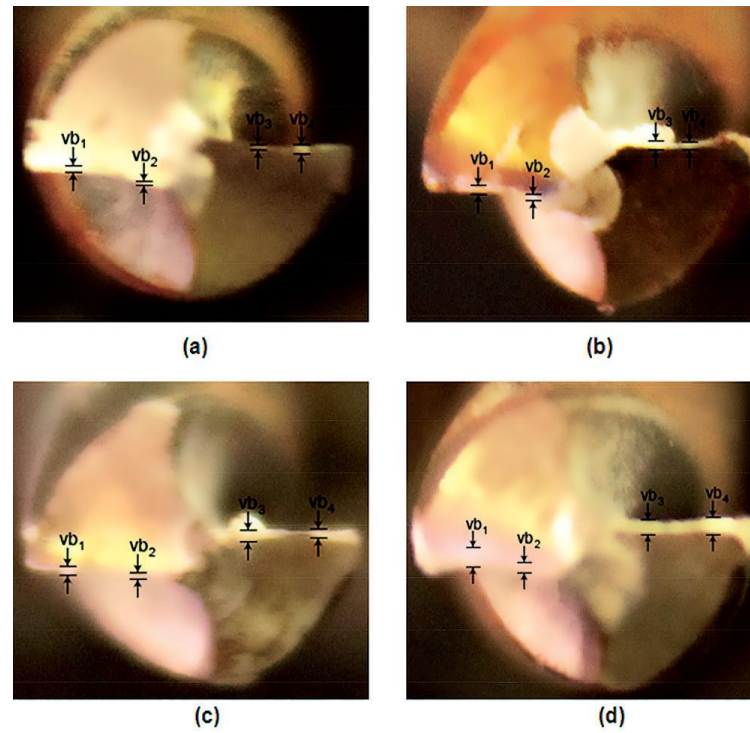
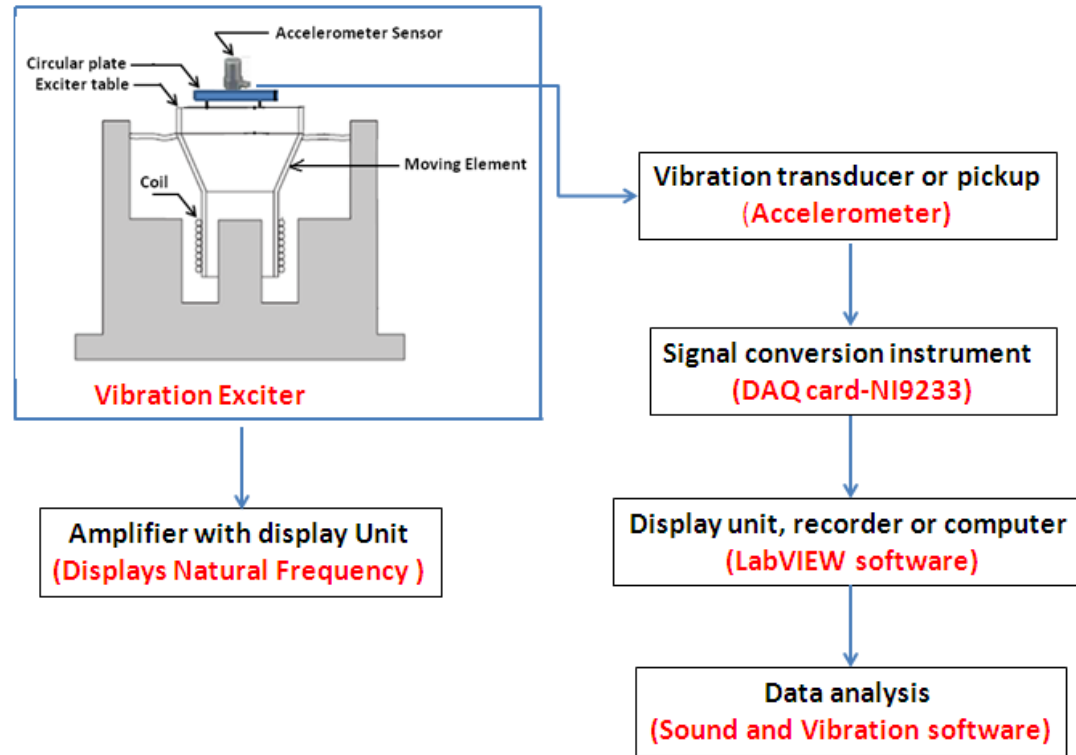


Figure 3: Flank wear measurement on tool tip



**Figure 4:** Flow chart of complete experiment process

The Gauge range of Taylor HolbsonSurtronic 128 is  $200\mu\text{m}/100\mu\text{m}/10\mu\text{m}$  which is used for hole surface measurement and monitoring of drilled holes. Maximum allowed surface roughness( $R_a$ ) value during drilling process is  $1.60\mu\text{m}$  as ASM standards.

## Results and Discussions

### Validation of Mathematical models

A comparative study of Eq (3), Eq (4) and the experimental values of flank wear has been reported in Table 5. Eq (4) is performing better than Eq (3) for all sets of variables. The highest deviation of Eq (3) from that of the experimental values of flank wear is 55% for the set ( $v = 1000$  rpm,  $f = 0.125$  mm/rev,  $d = 14$  mm), whereas, the same with that of Eq (4) has been recorded as 34%. Similarly, the highest deviation of Eq (4) with the experimental values of flank wear has been recorded for the following set ( $v = 900$  rpm,  $f = 0.089$  mm/rev,  $d = 9$  mm) as 35% whereas, Eq(3) results in 28% deviation for the same set. From the table, it is also evident that the overall average deviation of Eq (3) and Eq (4) from the experimental values was recorded as 22.66% and 17.26% respectively. A sharp reduction of 5% can be noticed, thus, proving the better performance of Eq (4) over Eq (3).Figure (5) shows the comparison between the values calculated by Eq (3), Eq (4) and the experimental values of flank wear.

**Table: 5** Comparison of flank wear values calculated by Eqs (3) & (4) and the experimental values

| v<br>(rev/min) | f<br>(mm/rev) | d<br>(mm) | $T_{p1}/T_{p2}$ | W (mm)   |          |          | Error %<br>Eq(3) &<br>Measured | Error %<br>Eq(4) &<br>Measured |
|----------------|---------------|-----------|-----------------|----------|----------|----------|--------------------------------|--------------------------------|
|                |               |           |                 | Measured | Eq (3)   | Eq (4)   |                                |                                |
| 800            | 0.089         | 9         | 18.2            | 0.22     | 0.218555 | 0.200456 | 3.7                            | 13.1                           |
| 800            | 0.089         | 11        | 34.6            | 0.32     | 0.316517 | 0.257925 | 14.6                           | 12.2                           |
| 800            | 0.089         | 14        | 40.4            | 0.36     | 0.347085 | 0.318315 | 27.7                           | 6.3                            |
| 800            | 0.125         | 9         | 13.2            | 0.21     | 0.183192 | 0.239208 | 25.4                           | 14.9                           |

|                 |       |    |      |       |          |          |      |      |
|-----------------|-------|----|------|-------|----------|----------|------|------|
| 800             | 0.125 | 11 | 17.5 | 0.276 | 0.216003 | 0.294596 | 28.4 | 21.8 |
| 800             | 0.125 | 14 | 23.2 | 0.32  | 0.255003 | 0.376395 | 26.7 | 23.3 |
| 800             | 0.15  | 9  | 10.7 | 0.21  | 0.163538 | 0.268686 | 53.4 | 29.7 |
| 800             | 0.15  | 11 | 15.4 | 0.256 | 0.201994 | 0.334097 | 27.7 | 14.7 |
| 800             | 0.15  | 14 | 13.6 | 0.292 | 0.190323 | 0.415375 | 7.0  | 26.0 |
| 900             | 0.089 | 9  | 13.9 | 0.24  | 0.18788  | 0.209129 | 27.9 | 35.5 |
| 900             | 0.089 | 11 | 39.1 | 0.364 | 0.340061 | 0.288771 | 23.5 | 13.2 |
| 900             | 0.089 | 14 | 47.3 | 0.487 | 0.380571 | 0.359218 | 12.0 | 2.4  |
| 900             | 0.125 | 9  | 13.7 | 0.232 | 0.187733 | 0.267371 | 18.8 | 1.2  |
| 900             | 0.125 | 11 | 32.4 | 0.344 | 0.307143 | 0.352528 | 26.5 | 17.6 |
| 900             | 0.125 | 14 | 48.4 | 0.461 | 0.387817 | 0.455586 | 23.3 | 15.0 |
| 900             | 0.15  | 9  | 15.5 | 0.256 | 0.20223  | 0.310906 | 19.7 | 13.6 |
| 900             | 0.15  | 11 | 25.6 | 0.333 | 0.26991  | 0.391944 | 20.0 | 4.6  |
| 900             | 0.15  | 14 | 44.6 | 0.445 | 0.371747 | 0.515543 | 6.3  | 14.9 |
| 1000            | 0.089 | 9  | 15.9 | 0.244 | 0.203288 | 0.233243 | 18.7 | 16.9 |
| 1000            | 0.089 | 11 | 38.7 | 0.36  | 0.33866  | 0.303287 | 26.9 | 24.3 |
| 1000            | 0.089 | 14 | 48.6 | 0.46  | 0.387272 | 0.393402 | 24.2 | 9.9  |
| 1000            | 0.125 | 9  | 11.8 | 0.22  | 0.173248 | 0.290822 | 21.6 | 10.0 |
| 1000            | 0.125 | 11 | 26.3 | 0.34  | 0.273686 | 0.377601 | 46.2 | 32.6 |
| 1000            | 0.125 | 14 | 43.3 | 0.444 | 0.365125 | 0.493792 | 55.2 | 34.0 |
| 1000            | 0.15  | 9  | 9.2  | 0.222 | 0.151814 | 0.329736 | 23.6 | 23.4 |
| 1000            | 0.15  | 11 | 11.4 | 0.268 | 0.172628 | 0.406157 | 3.7  | 13.1 |
| 1000            | 0.15  | 14 | 39.4 | 0.43  | 0.34787  | 0.561517 | 14.6 | 12.2 |
| Average Error % |       |    |      |       |          |          | 22.6 | 17.2 |

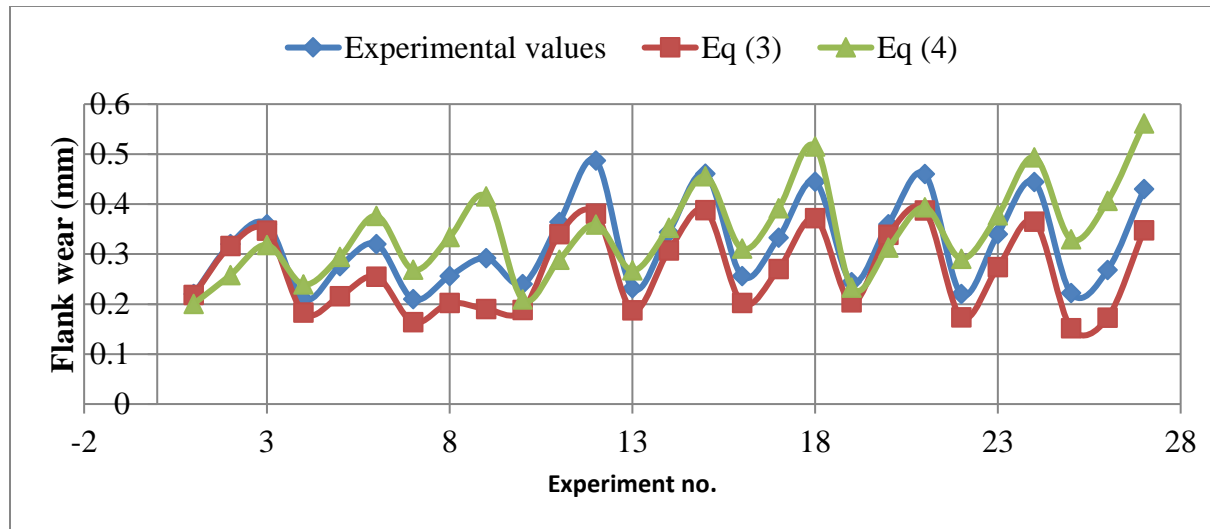


**Figure 5:** Comparison of Eq (3) and Eq (4) with experimental values of flank wear

### Optimization Results

The minimization of tool flank wear problem carried out for a single depth of cut ( $d = 11\text{mm}$ ) and 4 different speeds of spindle namely  $v = 850, 900, 950, 1000$  rpm. The optimum results are reported in the table (6). From tables 1 and 6 it is evident that the flank wear for 11 mm depth of cut has been reduced for the optimum parameters [22-26]. The flank wear value noticed for 11 mm depth of cut with 900 rpm as the speed of spindle and 0.089, 0.125, and 0.15 mm/rev are 0.364, 0.344, and 0.333 respectively. The reduction in flank wear through experiments is 41%, 38%, and 36% respectively. It is also clear from Table 6 that Eq. (4) is performing better than Eq. (3) even for optimum values. Table 7 lists the comparison of optimum results with that of the results reported

in Nakandhrakumar et al. 2019. Eq. (3) overestimates the flank wear values whereas Eq. (4) estimates appropriately.

Fig. 6 show the typical raw vibration signals in time domain accelerations and the corresponding frequency spectra while various wind velocities oscillate the different cross-sections of the mast in the range wind velocities from 3.7 m/s to 7.9 m/s. Therefore, all the observed vibration signals have been analyzed to extract their parameters in the time domain and frequency domain. As can be seen, the nature of the acquired vibration signal is complicated for categorizing using time-domain for various cross-sections being very similar across the record. This time trace approach produced nonlinearities in amplitude variations that arising out of excessive vibration as a result of the increase in wind velocities from the wind tunnel.

**Table 6:** Optimization results

| v<br>(rev/min) | f<br>(mm/rev) | d<br>(mm) | T <sub>p1</sub> /T <sub>p2</sub> | W (mm)   |          |          | Error %<br>Eq(3) &<br>Measured | Error %<br>Eq(4) &<br>Measured |
|----------------|---------------|-----------|----------------------------------|----------|----------|----------|--------------------------------|--------------------------------|
|                |               |           |                                  | Measured | Eq (3)   | Eq (4)   |                                |                                |
| 850            | 0.078         | 11        | 22                               | 0.195    | 0.244147 | 0.229595 | 20.1                           | 15.0                           |
| 900            | 0.0734        | 11        | 28                               | 0.212    | 0.28025  | 0.240634 | 24.3                           | 11.9                           |
| 950            | 0.079         | 11        | 30                               | 0.249    | 0.292071 | 0.266507 | 14.7                           | 6.5                            |
| 1000           | 0.079         | 11        | 65                               | 0.265    | 0.455086 | 0.301303 | 41.7                           | 17.5                           |

**Table 7:** Comparison of results

| v<br>(rev/min) | f<br>(mm/rev)     | d<br>(mm) | T <sub>p1</sub> /T <sub>p2</sub> | W (mm)                  |                                |                               |
|----------------|-------------------|-----------|----------------------------------|-------------------------|--------------------------------|-------------------------------|
|                |                   |           |                                  | Measured                | Eq (3)                         | Eq (4)                        |
| 900            | 0.089<br>(0.0734) | 11        | 39.1<br>(28)                     | 0.364<br>(0.212)<br>41% | 0.340061<br>(0.28025)<br>17%   | 0.288771<br>(0.24063)<br>16%  |
|                | 0.125<br>(0.0734) | 11        | 32.4<br>(28)                     | 0.344<br>(0.212)<br>38% | 0.307143<br>(0.28025)<br>8%    | 0.352528<br>(0.24063)<br>31%  |
|                | 0.15<br>(0.0734)  | 11        | 25.6<br>(28)                     | 0.333<br>(0.212)<br>36% | 0.26991<br>(0.28025)<br>-3%    | 0.391944<br>(0.24063)<br>38%  |
| 1000           | 0.089<br>(0.079)  | 11        | 38.6<br>(65)                     | 0.36<br>(0.265)<br>26%  | 0.33866<br>(0.45508)<br>-34%   | 0.303287<br>(0.30130)<br>3.8% |
|                | 0.125<br>(0.079)  | 11        | 26.3<br>(65)                     | 0.34<br>(0.265)<br>22%  | 0.273686<br>(0.45508)<br>-66%  | 0.377601<br>(0.30130)<br>20%  |
|                | 0.15<br>(0.079)   | 11        | 11.4<br>(65)                     | 0.268<br>(0.265)<br>1%  | 0.172628<br>(0.45508)<br>-163% | 0.406157<br>(0.30130)<br>25%  |

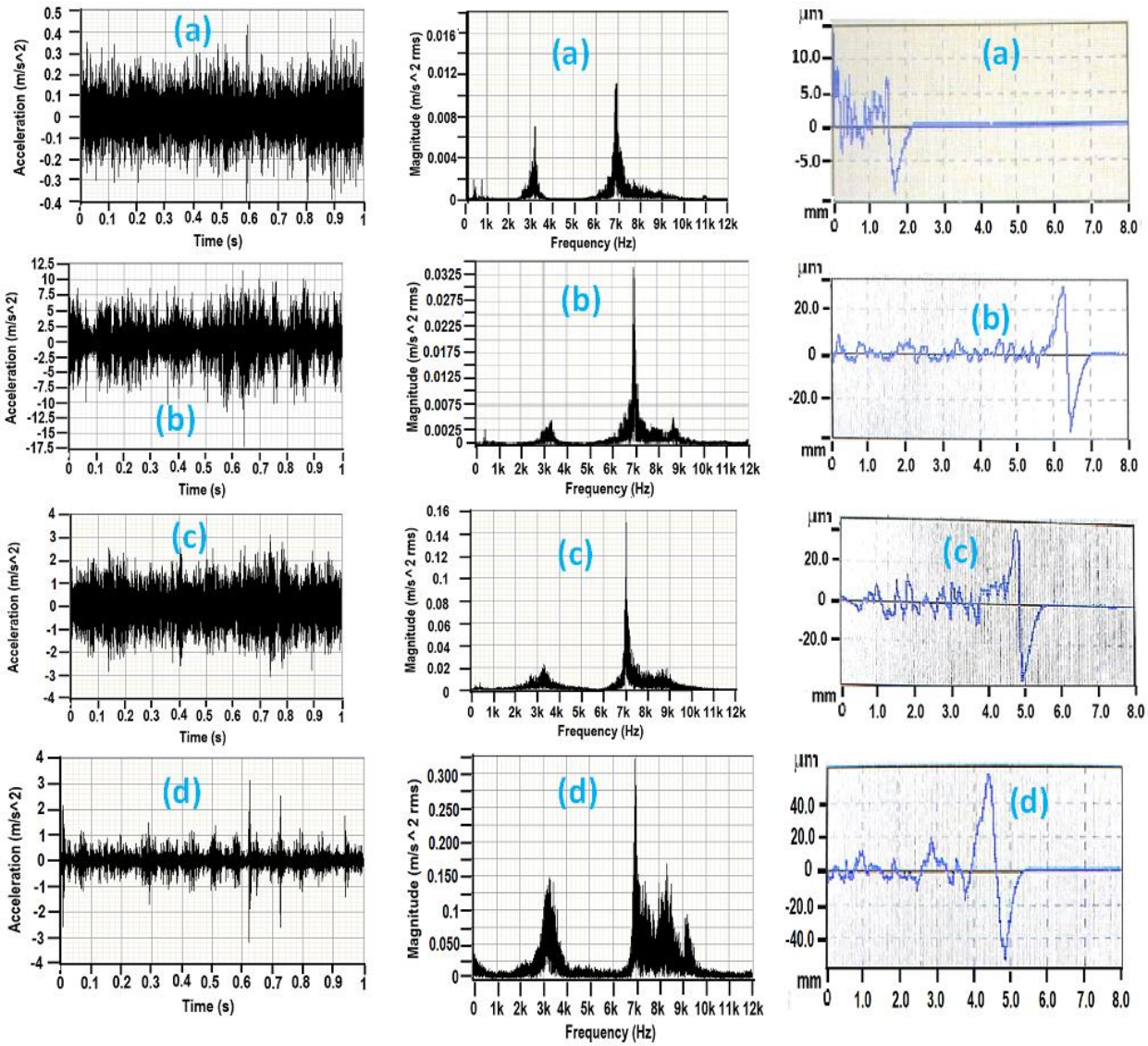


**Figure 6:** Time domain and their respective spectral plots of acceleration captured by accelerometer and corresponding surface roughness measured through Taylor HolbsonSurtronic 128 for cutting speed 850 rpm, feed 0.078mm/rev and doc 11 mm

- (a) Hole 10 – Time domain , FFT and surface roughness Ra ( $\mu\text{m}$ ) of 0.20
- (b) Hole 120 - Time domain , FFT and surface roughness Ra ( $\mu\text{m}$ ) of 0.80
- (c) Hole 240 - Time domain , FFT and surface roughness Ra ( $\mu\text{m}$ ) of 1.10
- (d) Hole 350 - Time domain , FFT and surface roughness Ra ( $\mu\text{m}$ ) of 1.70

Fig. 6 shows that Time domain signals and their corresponding Fast Fourier Transformation (FFT) plot received during experiments. Additionally during surface roughness plots are captured after drilling Hole number 10, 120, 240 and 350 by removing the plate from chuck. Measured values of RMS Amplitude in  $\text{m/s}^2$  and hole surface roughness ( $\mu\text{m}$ ) are tabulated in the Table 8. Surface roughness value reaches the maximum of 1.70  $\mu\text{m}$  during drilling hole number 350 and measured flank wear of drill is 0.46mm. Hence, no more holes are drilled. Drilling operation is stopped for the replacement of drill.

**Table 8:** RMS Amplitude of FFT plot and Surface roughness (Ra)

| Hole Number | RMS Amplitude ( $\text{m/s}^2$ ) in FFT plot | Surface Roughness (Ra – $\mu\text{m}$ ) |
|-------------|--|---|
| Hole10      | 0.011  | 0.20                                    |
| Hole 120    | 0.035  | 0.80                                    |
| Hole 240    | 0.15   | 1.10                                    |
| Hole 350    | 0.325  | 1.70                                    |

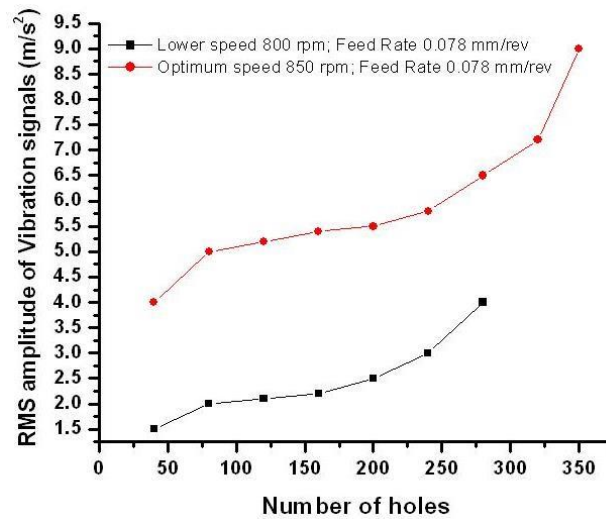


**Fig. 7. Graph to be plotted between number of holes and RMS Amplitude for two different cutting conditions**

Fig. 7 is plotted between number of holes drilled and RMS amplitude of vibration signals. Overall picture shows that while drilling carried with low speed of 800 rpm and feed rate 0.078 mm/rev, then maximum of 270 holes were drilled. At the same time drilling carried through optimum speed of 850 rpm and feed rate 0.078 mm/rev then maximum of holes drilled are increased upto 350.

During low speed conditions till 250 holes drill wear measured was 0.37mm. At the end drill wear increases suddenly to reach 0.45 mm of maximum drill wear. In the case of optimum speed condition, drill wear measured was 0.36mm till 325 holes and beyond 325 to 350 holes it's increases to 0.47 mm. So, optimum conditions help to drill more number of holes and which increases life of drill.

## Conclusion

In this work, a modified semi-empirical methodology has been reported for the computation of drill flank wear. This methodology is found to be more reliable for estimating drill flank wear than the previous methodology proposed by the authors. An optimization problem has been formulated to optimize the drilling operation parameters while considering the minimization of drill flank wear as the objective function. The results proved to be promising. The torsional-axial vibration amplitude ratio is a good indicator to predict and monitor the drill flank wear. Experiments also have been carried out successfully to validate the optimization results. During experiments, it is observed that the first peak ( $T_{p1}$ ) and the second peak ( $T_{p2}$ ) are highly sensitive to the drill flank wear and failure. Drill life increases while drilling carried with optimum cutting conditions according to the GA algorithm followed.

## References

1. Hashish, M. (1989) A Model for abrasive water jet machining. Transactions of ASME Journal of Engineering Materials and Technology , III, 154-162.
2. Kaye, J. E., Yan, D. H., Popplewell, N., and Balakrishnan, S., (1995) Predicting tool flank wear using spindle speed change, International Journal of Machine Tools & Manufacture, Vol. 35(9), pp. 1309-1320.
3. Cus, F., Sokovic, M., Kopac, J., and Balic, J., (1997) Model of complex optimization of cutting conditions", Journal of Materials Processing Technology, vol. 64, pp. 41-52.
4. Ertunc, H. M., and Lopara, K. A., (2001) A decision fusion algorithm for tool wear condition monitoring in drilling. International Journal of Machine Tools & Manufacture, Vol. 41, pp. 1347-1362.

5. Jen, T. C., Gutierrez, G., Eapen, S., Barber, G., Zhao, H., Szuba, P. S., Labataille, J., and Manjunathaiah, J., (2002) Investigation of heat pipe cooling in drilling applications. Part I: preliminary numerical analysis and verification. *International Journal of Machine Tools and Manufacture*, 42(5), 643-652.
6. Roukema, J. C., and Altintas, Y., (2004) Kinematic model of dynamic drilling process. ASME International Mechanical Engineering Congress and Exposition, Nov. 13-20, California, USA.
7. Al-sulaiman, F. A., Abdul Baseer, M., Sheikh A. K.,(2005) Use of electrical power for online monitoring of tool condition. *Journal of Materials Processing Technology*, 166, pp. 364-371.
8. Brozek, M., (2005) “cutting conditions optimization when turning overlays”, *Journal of Materials Processing Technology*, Vol. 168, pp. 488-495.
9. Dilbag Singh P. VenkateswaraRao., (2006), A surface roughness prediction model for hard turning process”, *Int. J Adv. Manuf. Technol.*, 32, pp. 1115-1124.
10. Roukema, J. C., and Altintas, Y., (2006) Time domain simulation of torsional-axial vibrations in drilling. *Int. Journal of Machine tools & manufacture*, 46, pp. 2073-2085.
11. Teti, R., Jemielniak, K., O’Donnell, G., and Dornfeld, D., (2010) Advanced monitoring of machining operations. *CIRP Annals – Manufacturing Technology*, 59, pp. 717 – 739.
12. Ratava, J., Lohtander, M., and Varis, J., (2017) Tool condition monitoring in interrupted cutting with acceleration sensors. *Robotics and Computer-Integrated Manufacturing*, 47, pp. 70-75.
13. Antic, A., Popovic, B., Krstanovic, L., Obradovic, R., and Milosevic, M., (2018) Novel texture-based descriptors for tool wear condition monitoring. *Mechanical systems and signal processing*, 98, pp. 1-15.
14. Deb, K.,(2014) *Multi-objective Optimization Using Evolutionary Algorithms*, Wiley India Pvt. Ltd., New Delhi, India.
15. AnupamAgrawal, SauravGoel, Waleed Bin Rashid, and Mark Price, (2015) Prediction of surface roughness during hard turning of AISI 4340 steel(69 HRC), *Applied Soft Computing*, 30, 279-286.
16. Vasudev, K. L., Sharma, R., and Bhattacharyya, S. K.,(2016) A modular and integrated optimization model for UVs, *DefenceSci. J.* 66 (1) 71–80.
17. Friedman, M. Y., and Field, M., (1974) Building of tool life models for use in a computerized numerical machining data bank, *Int. Conf. Prod. Engng.*, Tokyo, Part 1.

18. Nakandhrakumar, R. S., Dinakaran D., Pikton D., Patabiram J. (2019) Mathematical models of flank wear using vibration amplitude ratio in drilling. FME Transactions, Vol. 47, pp. 430-436.
19. Ketaki Joshi, Bhushan Patil, (2021) Prediction of Surface Roughness by Machine Vision using Principal Components based Regression Analysis, Procedia Computer Science, 167, pp. 382-391.
20. Suneel, K., Rao, N.N., Balaji, R., Srikanth, N., Solomon, G.R. and Selokar, A., 2020. Review on Sliding Wear of Ti-6Al-4V Alloy Concerning Counterface and Sliding Conditions. In Intelligent Manufacturing and Energy Sustainability (pp. 309-318). Springer, Singapore.
21. Abhishikt, C.B.N.S., Ramachandran, B. and Alekhya, G.N., 2020. Design and analysis of disk rotor brake under tribological behaviour of materials. Materials Today: Proceedings, 33, pp.4298-4310.
22. Balaji, R., Sivakumar, S., Nadarajan, M. and Selokar, A., 2019. A recent investigations: Effect of surface grinding on CFRP using rotary ultrasonic machining. Materials Today: Proceedings, 18, pp.5209-5218.
23. Kolisetty Aditya, V.E., Anish, P. and Samuel William, S., 2021. A Critical Investigation on Weld Bead Defect Detection System Using IoT. Turkish Journal of Computer and Mathematics Education (TURCOMAT), 12(14), pp.2047-2058.
24. Abitha, H., Kavitha, V., Gomathi, B. and Ramachandran, B., 2020. A recent investigation on shape memory alloys and polymers based materials on bio artificial implants-hip and knee joint. Materials Today: Proceedings, 33, pp.4458-4466.
25. Balaji, R., Nadarajan, M., Selokar, A., Kumar, S.S. and Sivakumar, S., 2019. Modelling and analysis of disk brake under tribological behaviour of Al-Al<sub>2</sub>O<sub>3</sub> ceramic matrix composites/Kevlar<sup>®</sup> 119 composite/C/SiC-carbon matrix composite/Cr-Ni-Mo-V steel. Materials Today: Proceedings, 18, pp.3415-3427.
26. Amir, M., Tu, S., Tolouei-Rad, M., Giasin, K. and Vafadar, A., 2020. Optimization and modeling of process parameters in multi-hole simultaneous drilling using taguchi method and fuzzy logic approach. Materials, 13(3), p.680.